JOURNAL OF THEORETICAL
AND APPLIED MECHANICS
44, 4, pp. 767-782, Warsaw 2006

MODELING OF STRAIN LOCALIZATION IN QUASI-BRITTLE MATERIALS WITH A COUPLED ELASTO-PLASTIC-DAMAGE MODEL

Jerzy Bobiński
Jacek Tejchman

Faculty of Civil and Environmental Engineering, Gdansk University of Technology
e-mail: bobin@pg.gda.pl; tejchmk@pg.gda.pl

The paper presents results of numerical simulations of strain localization in quasi-brittle materials (like concrete) under plane strain conditions. To model the material behaviour, an isotropic elasto-plastic-damage model combining elasto-plasticity and scalar damage was used. An elasto-plastic constitutive law using a Drucker-Prager yield surface (in compression) and Rankine yield surface (in tension) was defined. A modified failure criterion by Rankine for the equivalent strain using an exponential evolution law was assumed within damage mechanics. To obtain mesh-independent results of strain localization, the model was enhanced by non-local terms in the softening regime. A four-point bending test of a concrete beam with a single notch was numerically simulated using the finite element method. FE-results were compared with laboratory experiments.

Key words: damage mechanics, elasto-plasticity, non-local theory, strain localization

1. Introduction

Analysis of concrete elements is complex due to occurrence of strain localization which is a fundamental phenomenon under both quasi-static and dynamic conditions (Bazant, 1984, 2003; Wittmann *et al.*, 1992; van Vliet and van Mier, 1996; Chen *et al.*, 2001). It can occur in the form of cracks (if cohesive properties are dominant) or shear zones (if frictional properties prevail). The determination of the width and spacing of strain localization is crucial to evaluate the material strength at peak and in the post-peak regime. Concrete behaviour can be modeled within continuum mechanics models using e.g.: non-linear elasticity (Palaniswamy and Shah, 1974), fracture (Bazant and

Cedolin, 1979; Hilleborg, 1985), endochronic theory (Bazant and Bhat, 1976; Bazant and Shieh, 1978), micro-plane theory (Bazant and Ozbolt, 1990; Jirasek, 1999), plasticity (Willam and Warnke, 1975; Pietruszczak *et al.*, 1988; Menetrey and Willam, 1995; Bobinski and Tejchman, 2004), damage theory (Dragon and Mroz, 1979; Peerlings *et al.*, 1998; Chen, 1999; Bobinski and Tejchman, 2005) and the coupled plastic-damage approach (Lemaitre, 1985; de Borst *et al.*, 1999; Ibrahimbegovic *et al.*, 2003, Salari *et al.*, 2004), as well as discrete models using the lattice approach (Herrmann *et al.*, 1989; Vervuurt *et al.*, 1994; Schlangen and Garboczi, 1997; Kozicki and Tejchman, 2006a) and DEM (Sakaguchi and Mühlhaus, 1997; D'Addetta *et al.*, 2002; Donze *et al.*, 1999). To properly describe the strain localization within continuum mechanics, the models should be enhanced by the characteristic length of a micro-structure (de Borst *et al.*, 1992; Chen *et al.*, 2001). There are several approaches within continuum mechanics to include the characteristic length and to preserve well-posedness of the underlying incremental boundary value problem (de Borst *et al.*, 1992) in quasi-brittle materials as: second-gradient (Chen *et al.*, 2001; Peerlings *et al.*, 1998; Pamin and de Borst, 1998; Pamin, 2004), non-local (Pijaudier-Cabot and Bazant, 1987; Chen, 1999; Akkermann, 2000; Bobinski and Tejchman, 2004; Jirasek, 2004), and viscous ones (Sluys, 1992; Sluys and de Borst, 1994). Owing to them, objective and properly convergent numerical solutions for localized deformation (mesh-insensitive load-displacement diagram and mesh-insensitive deformation pattern) are achieved. Otherwise, FE-results are completely controlled by the size and orientation of the mesh, and thus produce unreliable results, i.e. strain localization becomes narrower upon mesh refinement (element size becomes the characteristic length) and computed force-displacement curves change considerably depending on the width of the calculated localization. In addition, a premature divergence of incremental FE-calculations is often met.

The aim of the present paper is to show the capability of an isotropic elasto-plastic-damage continuum model to describe the strain localization and stiffness degradation in a concrete element during monotonous and cyclic four-point bending. The model is enhanced by the internal length of a micro-structure in the softening regime by means of non-local theory. The FE-results are compared to corresponding laboratory experiments by Hordijk (1991). The paper is a continuation of FE-investigations of the strain localization in concrete elements performed with the elasto-plastic model with non-local softening (Bobiński and Tejchman, 2004, 2006) and the non-local damage model with non-local softening (Bobiński and Tejchman 2005). These investigations have shown that the non-local theory allows us to obtain fully objective numerical solutions for boundary value problems including the strain localization.

2. Constitutive continuum model

2.1. Isotropic elasto-plastic model

An elasto-plastic model with the isotropic hardening and softening consists of two yield conditions. In the compression regime, the linear Drucker-Prager criterion is defined as (Abaqus, 1998; Bobinski and Tejchman, 2004, 2006)

$$f_1 = q + p\tan\varphi - \Big(1 - \frac{1}{3}\tan\varphi\Big)\sigma_c(\kappa_1) \tag{2.1}$$

wherein q is the von Mises equivalent stress, p – mean stress, φ – internal friction angle, σ_c – uniaxial compression yield stress, κ_1 – hardening (softening) parameter equal to plastic strain in uniaxial compression ε^p_{11}. The invariants p and q are

$$p = \frac{1}{3}\sigma_{kk} \qquad \text{and} \qquad q = \sqrt{\frac{3}{2}s_{ij}s_{ji}} \tag{2.2}$$

where σ_{ij} – stress tensor and s_{ij} – deviatoric stress tensor. The flow potential function is taken as

$$g_1 = q + p\tan\psi \tag{2.3}$$

where ψ denotes the dilatancy angle. The flow rule is assumed as

$$d\varepsilon^p_{ij} = \frac{d\kappa_1}{1 - \frac{1}{3}\tan\psi}\frac{\partial g_1}{\partial\sigma_{ij}} \tag{2.4}$$

In the tensile regime, the Rankine criterion is assumed (Bobinski and Tejchman, 2006) with the yield function

$$f_2 = \max\{\sigma_1, \sigma_2, \sigma_3\} - \sigma_t(\kappa_2) \tag{2.5}$$

where σ_1, σ_2 and σ_3 denote the principal stresses, σ_t – tensile yield stress and κ_2 – hardening (softening) parameter (equal to the maximum principal plastic strain ε^p_1). The associated flow rule is assumed. To model the concrete softening in tension, the exponential curve by Hordijk (1991) is chosen

$$\sigma_t(\kappa_2) = f_t[(1 + A_1\kappa_2^3)\exp(-A_2\kappa_2) - A_3\kappa_2] \tag{2.6}$$

where f_t stands for the tensile strength of the concrete. The constants A_1, A_2 and A_3 are

$$A_1 = \frac{c_1}{\kappa_u} \qquad A_2 = \frac{c_2}{\kappa_u} \qquad A_3 = \frac{1}{\kappa_u}(1 + c_1^3)\exp(-c_2) \tag{2.7}$$

where κ_u denotes the ultimate value of the softening parameter, $c_1 = 3$ and $c_2 = 6.93$.

The constitutive isotropic elasto-plastic model for concrete requires two elastic parameters: modulus of elasticity E and Poisson's ratio ν, one compresion plastic function $\sigma_c = f(\kappa_1)$, one tensile plastic function $\sigma_t = f(\kappa_2)$, internal friction angle φ and dilatancy angle ψ.

2.2. Isotropic damage model

The model describes degradation of a material due to micro-cracking with the aid of a single scalar damage parameter D growing from zero (undamaged state) to one (completely damaged state) (Bobinski and Tejchman, 2005). The stress-strain relationship is represented by the following relationship

$$\sigma_{ij} = (1 - D)C^e_{ijkl}\varepsilon_{kl} \tag{2.8}$$

where C^e_{ijkl} is the linear elastic material stiffness matrix and ε_{kl} – strain tensor. The damage parameter D acts as a stiffness reduction factor (Poisson's ratio is not affected by damage and it remains constant). The growth of the damage variable is controlled by the damage threshold parameter κ, which is defined as the maximum of the equivalent strain measure $\widetilde{\varepsilon}$ reached during the load history up to time t

$$\kappa = \max_{\tau \leqslant t} \widetilde{\varepsilon}(\tau) \tag{2.9}$$

The loading function of damage is equal to

$$f(\widetilde{\varepsilon}, \kappa) = \widetilde{\varepsilon} - \max\{\kappa, \kappa_0\} \tag{2.10}$$

where κ_0 is the initial value of κ when damage starts. If the loading function f is negative, damage does not develop. During monotonic loading, the parameter κ grows (it coincides with $\widetilde{\varepsilon}$) and during unloading and reloading it remains constant. To describe the equivalent strain measure $\widetilde{\varepsilon}$, a definition corresponding to the Rankine failure criterion (Jirasek, 2004) is adopted

$$\widetilde{\varepsilon} = \frac{1}{E} \max\{\sigma^{eff}_i\} \tag{2.11}$$

where E is the modulus of elasticity and σ^{eff}_i are the principal values of the effective stress σ^{eff}_{ij}

$$\sigma^{eff}_{ij} = C^e_{ijkl}\varepsilon^e_{kl} \tag{2.12}$$

To describe the evolution of the damage parameter D, an exponential softening law proposed by Peerlings *et al.* (1999) is assumed

$$D = 1 - \frac{\kappa}{\kappa_0}\Big(1 - \alpha + \alpha e^{-\beta(\kappa - \kappa_0)}\Big) \tag{2.13}$$

where α and β are material parameters.

The constitutive isotropic damage model for concrete requires the following parameters: modulus of elasticity E, Poisson's ratio ν, f_t, κ_0, α and β.

2.3. Coupled elasto-plastic damage model

This model combines elasto-plasticity with scalar damage enhanced by non-locality and enables one to simulate the stiffness degradation during cyclic loading due to cracks and plastic strains. It follows the second-gradient model formulated by Pamin and de Borst (1999). It assumes that the total strains ε_{ij} are equal to strains in an undamaged skeleton ε_{ij}^{eff} (effective strains). The plastic flow can occur only in the undamaged specimen, so the elasto-plastic model is defined in terms of effective stresses (Eq. (2.11)). As a consequence, the damage degradation does not affect plasticity. Equation (2.8) is modified as

$$\sigma_{ij} = (1-D)\sigma_{ij}^{eff} = (1-D)C_{ijkl}^{e}\varepsilon_{kl}^{e} \tag{2.14}$$

First, elasto-plastic calculations in the effective stress space are performed. After that the damage parameter D is calculated. The equivalent strain measure $\widetilde{\varepsilon}$ (Eq. (2.11)) can be defined in terms of the total strain ε_{ij} or in terms of the elastic strain ε_{ij}^{e}. In the first case, the equivalent strain measure $\widetilde{\varepsilon}$ (Eq. (2.11)) is obtained by replacing the elastic strain ε_{ij}^{e} by the total strain ε_{ij} only in Eq. (2.12). Finally, the stresses are obtained according to Eq. (2.14).

3. Non-local theory

To describe the strain localization, to preserve well-posedness of the boundary value problem and to obtain mesh-independent FE-results, a non-local theory was used as a regularization technique (Pjaudier-Cabot and Bazant, 1987; Bobinski and Tejchman, 2004). Usually, it is sufficient to treat non-locally only the variable controlling the material softening (Brinkgreve, 1994) (whereas stresses and strains remain local). It is assumed in elasto-plasticity that the softening parameter κ was non-local (Bobinski and Tejchman, 2004)

$$\overline{\kappa}(x_k) = \frac{1}{A}\int \omega(r)\kappa(x_k + r)\,dV \qquad \text{with} \qquad A = \int \omega(r)\,dV \tag{3.1}$$

where x_k are the coordinates of the considered (actual) point, r – distance measured from the point x_k to other material points, ω – weighting function and A – weighted volume. As a weighting function ω, the Gauss distribution function for 2D problems is used

$$\omega(r) = \frac{1}{l\sqrt{\pi}}\exp\Big[-\Big(\frac{r}{l}\Big)^2\Big] \tag{3.2}$$

where l denotes the characteristic (internal) length connected to the microstructure of the material. The averaging in Eq. (3.1) is restricted to a small representative area around each material point. The influence of points at the distance of $r = 3l$ is only about 0.1% (Fig. 1). The softening rates $d\kappa_i$ are assumed according to the modified formula (Brinkgreve, 1994) (independently for both yield surfaces)

$$d\overline{\kappa}_i(x_k) = (1-m)d\kappa_i(x_k) + \frac{m}{A}\int [\omega(r)d\kappa_i(x_k+r)]\, dV \tag{3.3}$$

where m is the additional material parameter which should be greater than 1 to obtain mesh-independent results (Bobinski and Tejchman, 2004). Eq. (3.3) can be rewritten as (Brinkgreve, 1994)

$$d\overline{\kappa}_i(x_k) = d\kappa_i(x_k) + m\Big(\frac{1}{A}\int [\omega(r)d\kappa_i(x_k+r)]\, dV - d\kappa_i(x_k)\Big) \tag{3.4}$$

Since the rates of the hardening parameter are not known at the beginning of each iteration, extra sub-iterations are required to solve Eq. (3.4). To simplify the calculations, the non-local rates are replaced by their approximations $d\kappa_i^{est}$ calculated on the basis of the known total strain rates (Brinkgreve, 1994)

$$d\overline{\kappa}_i(x_k) \approx d\kappa_i(x_k) + m\Big(\frac{1}{A}\int [\omega(r)d\kappa_i^{est}(x_k+r)]\, dV - d\kappa_i^{est}(x_k)\Big) \tag{3.5}$$

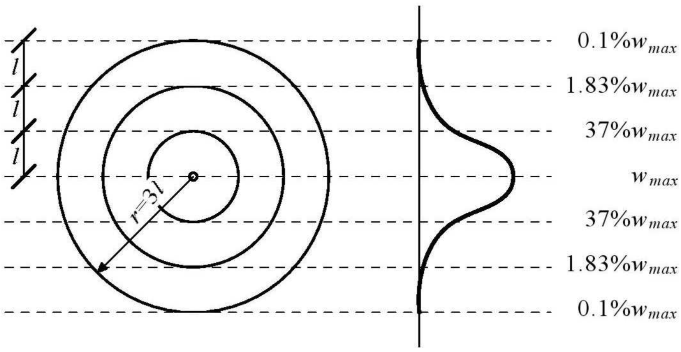

Fig. 1. Region of the influence of the characteristic length l and weighting function w

In the damage mechanics model, the equivalent strain measure $\widetilde{\varepsilon}$ is replaced in Eq. (2.11) by its non-local definition $\overline{\varepsilon}$

$$\overline{\varepsilon}(x_k) = \frac{1}{A}\int \omega(r)\widetilde{\varepsilon}(x_k+r)\, dV \tag{3.6}$$

In the coupled elasto-plastic-damage model, the non-locality can be introduced in elasto-plasticity or in damage. All three non-local models were implemented in the Abaqus Standard program (Abaqus, 1999) with the aid of the subroutine UMAT (user constitutive law definition) and UEL (user element definition) (Bobinski and Tejchman, 2004, 2005, 2006). The FE-simulations were performed under plane strain conditions. A geometric nonlinearity (large displacements) was taken into account. A quadrilateral elements composed of four diagonally crossed triangles were used to avoid volumetric locking (Groen, 1997).

4. FE-simulations

The problem of a notched beam under four-point bending was experimentally investigated by Hordijk (1991) and numerically simulated both by Pamin (1994) with a second-gradient elasto-plastic model and by Simone *et al.* (2002) with a second-gradient damage model. The geometry of the specimen is given in Fig. 2. The beam has a small notch $(5 \times 10\,\mathrm{mm}^2)$ at the mid-span. The thickness of the beam is 50 mm. The deformation is induced by imposing a vertical displacement of $\Delta v = 0.25$ mm at two nodes at the top in the central part of the beam. The FE-calculations are carried out under plane strain conditions. The modulus of elasticity is assumed to be $E = 40$ GPa and Poisson's ratio $\nu = 0.2$. FE-analyses are carried out with 3 different meshes: coarse (2152 triangular elements), medium (2332 triangular elements) and fine (4508 triangular elements) mesh (Fig. 3).

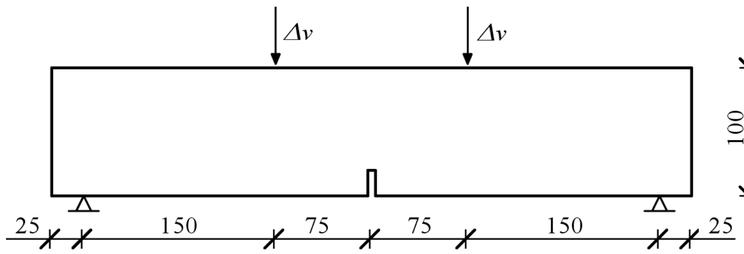

Fig. 2. Geometry and boundary conditions of the notched beam under bending [mm]

Figure 4 shows load-displacement curves for different meshes with the elasto-plastic model using non-local softening. The plastic tensile curve is assumed according to Eqs. (2.6) and (2.7) with $f_t = 2.3$ MPa and $\kappa_u = 7 \cdot 10^{-3}$. The plastic material parameters in a compression regime has not any influence on the FE-results. The characteristic length is taken as $l = 10$ mm and the parameter $m = 2$. The calculated curves in Fig. 4 are similar for all FE-meshes and are in a good agreement with the experimental outcome (Hordijk, 1991).

In the case of the coupled elasto-plastic-damage model, the calculations have been carried out only with the hardening elasto-plastic model combined

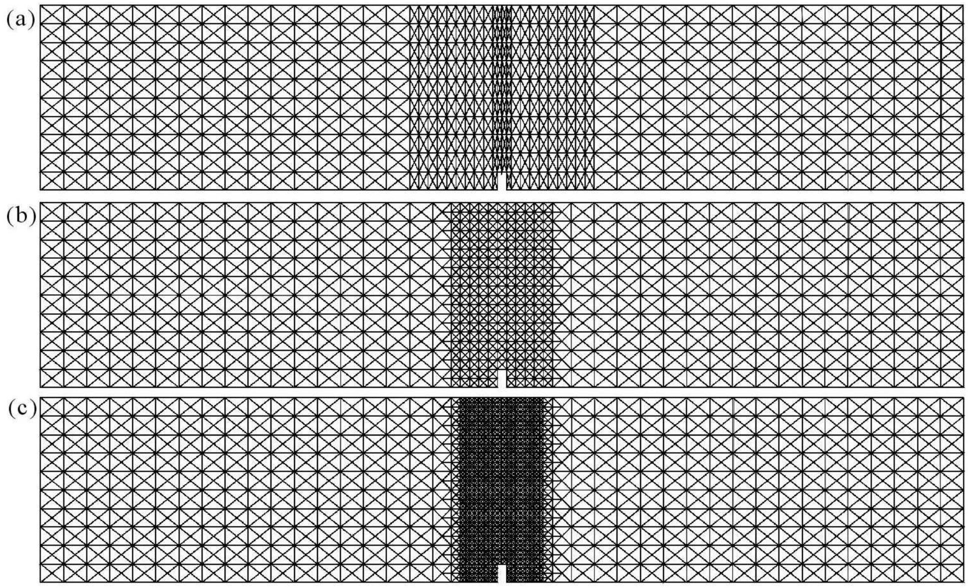

Fig. 3. FE-meshes used in numerical simulations: coarse (a), medium (b) and fine mesh (c)

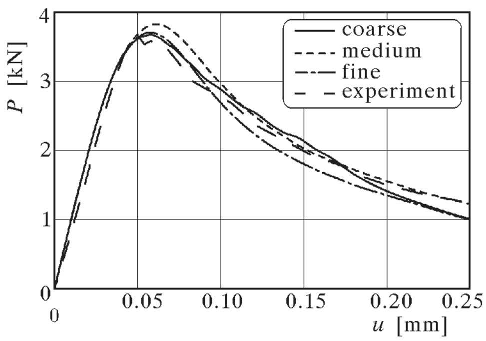

Fig. 4. Calculated load-displacement curves for a beam under four-point bending for different meshes using the elasto-plastic model with non-local softening compared to the experiment (Hordijk, 1991)

with damage, which has a better physical motivation (on the basis of the FE-results by Pamin and de Borst (1999)). The crucial point is to obtain the start of damage and yielding almost at the same time. In the first step, for the sake of simplicity, the von Mises yield criterion with the yield stress $\sigma_y = 4.5\,\mathrm{MPa}$ and a linear hardening parameter (with the modulus $h_p = E/2$) are defined in the compression regime. In the damage regime, the following parameters are assumed: $\kappa_0 = 4.6 \cdot 10^{-5}$, $\alpha = 0.92$, $\beta = 200$ and $l = 5\,\mathrm{mm}$.

Figure 5 shows load-displacement diagrams for the damage model and the coupled elasto-plastic-damage model with the equivalent strain measure as the total strain and as the elastic strain. The damage model well agrees with the experimental curve, while the curve calculated with the coupled model with the total strain $\widetilde{\varepsilon}(\varepsilon_{ij})$ lies under, and the curve computed with the coupled model with the elastic strain $\widetilde{\varepsilon}(\varepsilon^e_{ij})$ lies above the experimental curve.

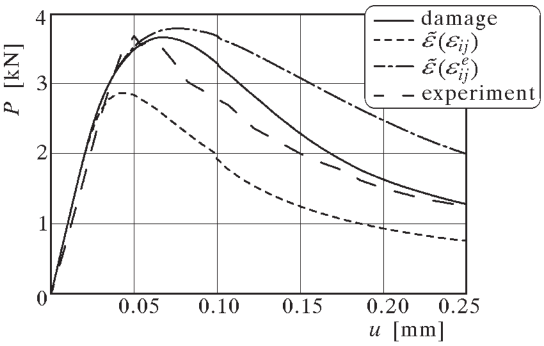

Fig. 5. Load-displacement curves for the damage model and coupled elasto-plastic-damage models using the total and elastic strains ($\kappa_0 = 4.6 \cdot 10^{-5}$, $\alpha = 0.92$, $\beta = 200$ and $l = 5\,\mathrm{mm}$)

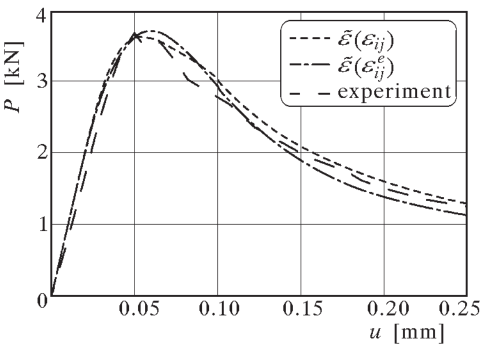

Fig. 6. Simulated load-displacement curves for the coupled elasto-plastic-damage model with non-local softening using the total strain ($\kappa_0 = 6 \cdot 10^{-5}$, $\beta = 150$, $l = 5\,\mathrm{mm}$) and the elastic strain ($\kappa_0 = 5 \cdot 10^{-5}$, $\beta = 400$, $l = 5\,\mathrm{mm}$) compared to the experiment by Hordijk (1991)

To obtain a better agreement with experiments, new material parameters have been calibrated for the coupled elasto-plastic-damage model. The following new parameters κ_0 and β have been chosen ($l = 5\,\mathrm{mm}$): $\kappa_0 = 6 \cdot 10^{-5}$ and $\beta = 150$ for the model with the equivalent strain measure equal to the total strain, and $\kappa_0 = 5 \cdot 10^{-5}$ and $\beta = 400$ for the model with the equivalent strain measure equal to the elastic strain. The improved load-displacement curves are presented in Fig. 6. An insignificant effect of the mesh discretization on the load-displacement curves is demonstrated in Fig. 7.

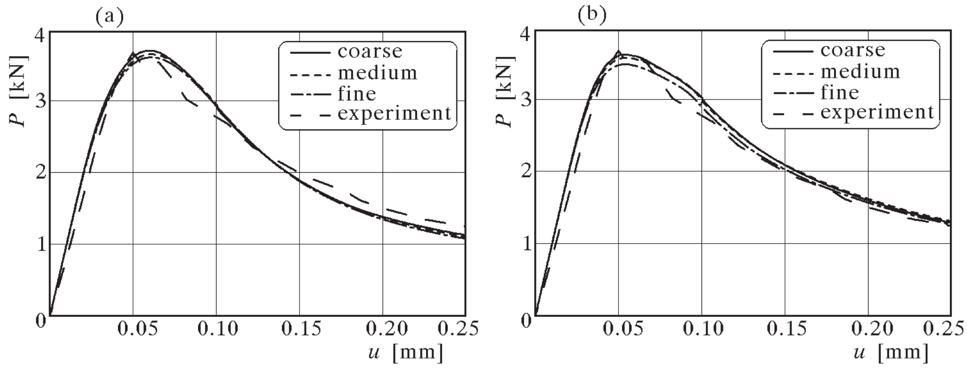

Fig. 7. Calculated load-displacement curves for different meshes (Fig. 3) with the coupled elasto- plastic-damage model with non-local softening using the elastic ($\kappa_0 = 6 \cdot 10^{-5}$, $\beta = 150$, $l = 5$ mm) (a) and the total strain ($\kappa_0 = 5 \cdot 10^{-5}$, $\beta = 400$, $l = 5$ mm) (b) compared to the experiment by Hordijk (1991)

The calculated contours of the non-local parameter κ above the notch are shown in Fig. 8 for three models. The obtained results do not depend on the mesh size. The width of the localized zone is approximately equal to 25 mm ($2.5 \times l$) within elasto-plasticity, 31 mm ($6.2 \times l$) in damage mechanics, and 31 mm ($6.2 \times l$) within elasto-plasticity combined with damage.

A comparison with the experimental result by Hordijk (1991) for a beam subject to cycling loading has also been performed. Figures 9 and 10 show the obtained curves for the coupled elasto-plastic-damage model with total strains $\widetilde{\varepsilon}(\varepsilon_{ij})$ and elastic strains $\widetilde{\varepsilon}(\varepsilon_{ij}^e)$, respectively, using the improved set of the material parameters. The result with the coupled elasto-plastic damage model using total strains $\widetilde{\varepsilon}(\varepsilon_{ij})$ fits the experimental outcome (load reversals exhibit a proper gradual increase of the elastic stiffness degradation), whereas the results with the coupled elasto-plastic damage model using elastic strains $\widetilde{\varepsilon}(\varepsilon_{ij}^e)$ slightly overestimate the grade of the stiffness degradation. To obtain more accurate results in the second case, further improvement of the material parameters is needed again.

The obtained FE-results with the non-local model are quantitatively in good agreement with corresponding numerical results by Pamin and de Borst (1999) obtained for the second-gradient elasto-plastic-damage model. Both the shape of load-displacements curves and the width of localized zones are similar. Thus, the non-local model is as effective as the second-gradient model in the numerical description of strain localization.

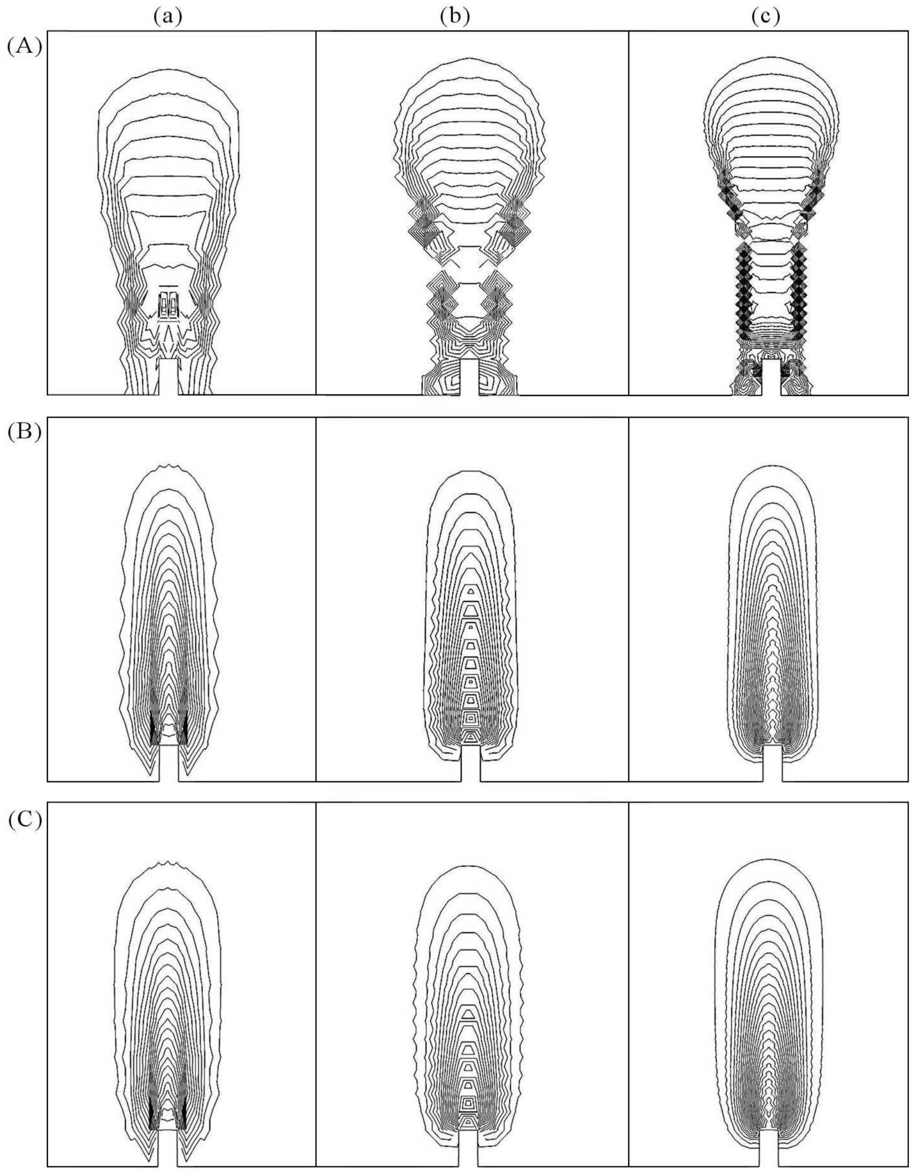

Fig. 8. Calculated contours of the non-local parameter κ near the notch for a beam under four-point bending for different FE-meshes (a) coarse, (b) medium and (c) fine mesh and different models (A) elasto-plasticity, (B) damage, (C) elasto-plasticity-damage (with elastic strains)

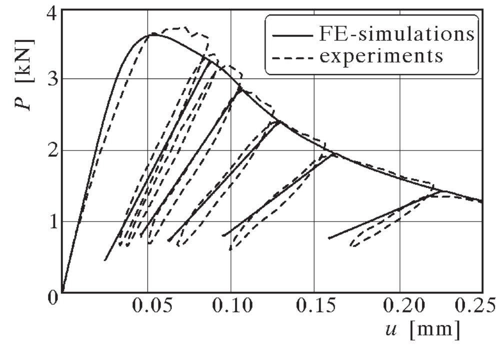

Fig. 9. Calculated load-displacement curves for the coupled elasto-plastic-damage model with non-local softening using the total strain ($\kappa_0 = 6 \cdot 10^{-5}$, $\beta = 150$, $l = 5\,\mathrm{mm}$) during cycling beam loading

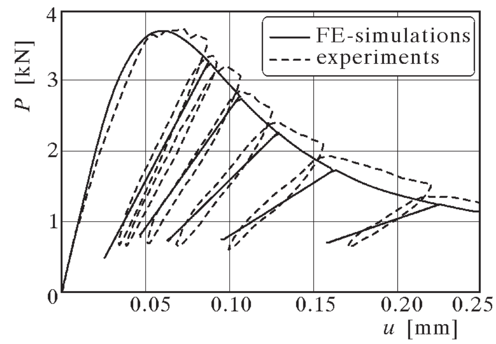

Fig. 10. Calculated load-displacement curves for the coupled elasto-plastic-damage model with non-local softening using the elastic strain ($\kappa_0 = 5 \cdot 10^{-5}$, $\beta = 400$, $l = 5\,\mathrm{mm}$) during cycling beam loading

5. Conclusions

The FE-calculations show that the hardening isotropic elasto-plastic model with softening isotropic damage enhanced by the characteristic length of a micro-structure can properly reproduce the experimental load-displacement diagrams and strain localization in quasi-brittle materials during monotonic and cyclic bending. During cycling loading, the fully coupled elasto-plastic damage model with few model parameters is able to reflect both the stiffness degradation and the irreversible strains. The FE-results with respect to the load-displacement curve and width of strain localization do not suffer from mesh sensitivity. The most realistic results are obtained with the equivalent strain measure assumed as the total strain. The calculated width of the localized zone in the concrete element is larger for the damage model and elasto-plastic model combined with damage ($6.2 \times l$) than with the elasto-plastic model ($2.5 \times l$) for the same characteristic length.

Numerical calculations of strain localization in concrete elements with the coupled model will be continued in further research. In the compressive regime, the more advanced elasto-plastic model by Menetrey and Willam (1995) will be used. A spatially correlated distribution of the tensile strength will be assumed (Walukiewicz *et al.*, 1997; Tejchman, 2006). In addition, laboratory tests will be performed wherein the width of the localized zone will be measured in beams using the DIC technique (Bhandari and Inoue, 2005; Kozicki and Tejchman, 2006b).

Acknowledgments
The numerical calculations were carried out on supercomputers at the Academic Computer Centre in Gdansk TASK.

References

1. Abaqus *Theory Manual*, Version 5.8, 1998, Hibbit, Karlsson & Sorensen Inc.
2. Akkermann J., 2000, *Rotationsverhalten von Stahlbeton-Rahmenecken*, Dissertation, Universitat Fridericiana zu Karlsruhe, Karlsruhe
3. Bazant Z.P., 1984, Size effect in blunt fracture: concrete, rock, metal, *J. Eng. Mech. ASCE*, **110**, 518-535
4. Bazant Z.P., 2003, *Scaling of Structural Strength*, Hermes-Penton, London
5. Bazant Z.P., Bhat P.D., 1976, Endochronic theory of inelasticity and failure of concrete, *J. Eng. Mech. Div. ASCE*, **102**, 701-722
6. Bazant Z.P., Cedolin L., 1979, Blunt crackband propagation in finite element analysis, *J. Eng. Mech. Div. ASCE*, **105**, 2, 297-315
7. Bazant Z.P., Ozbolt J., 1990, Non-local microplane model for fracture, damage and size effect in structures, *J. Eng. Mech. ASCE*, **116**, 2485-2505
8. Bazant Z.P., Shieh C.L., 1978, Endochronic model for nonlinear triaxial behaviour of concrete, *Nucl. Engng. Des.*, **47**, 305-315
9. Bhandari A.R., Inoue J., 2005, Experimental study of strain rates effects on strain localization characteristics of soft rocks, *Soils and Foundations*, **45**, 1, 125-140
10. Bobinski J., Tejchman J., 2004, Numerical simulations of localization of deformation in quasi-brittle materials within non-local softening plasticity, *Computers and Concrete*, **4**, 433-455
11. Bobinski J., Tejchman J., 2005, Modelling of concrete behaviour with a non-local continuum damage approach, *Archives of Hydro-Engineering and Environmental Mechanics*, **52**, 1, 85-102

12. Bobinski J., Tejchman J., 2006, Modelling of size effects in concrete using elasto-plasticity with non-local softening, *Archives of Civil Engineering*, **LII**, 1, 7-35

13. de Borst R., Mühlhaus H.-B, Pamin J., Sluys L., 1992, Computational modelling of localization of deformation, In: *Proc. of the 3rd Int. Conf. Comp. Plasticity*, D.R.J. Owen, H. Onate, E. Hinton (edit.), Swansea, Pineridge Press, 483-508

14. de Borst R., Pamin J., Geers M., 1999, On coupled gradient-dependent plasticity and damage theories with a view to localization analysis, *Eur. J. Mech. A/Solids*, **18**, 6, 939-962

15. Brinkgreve R.B.J., 1964, *Geomaterical models and numerical analysis of softening*, PhD Thesis, Delft University of Technology

16. Chen E., 1999, Non-local effects on dynamic damage accumulation in brittle solids, *I. J. Num. Anal. Meth. Geomech.*, **23**, 1-21

17. Chen J., Yuan H., Kalkhof D., 2001, A nonlocal damage model for elastoplastic materials based on gradient plasticity theory, *Report Nr.01-13*, Paul Scherrer Institut, 1-130

18. D'Addetta G.A., Kun F., Ramm E., 2002, In the application of a discrete model to the fracture process of cohesive granular materials, *Granular Matter*, **4**, 77-90

19. Donze F.V., Magnier S.A., Daudeville L., Mariotti C., Davenne L., 1999, Numerical study of compressive behaviour of concrete at high strain rates, *J. Eng. Mechanics*, 1154-1163

20. Dragon A., Mroz Z., 1979, A continuum model for plastic-brittle behaviour of rock and concrete, *Int. J. Eng. Science*, **17**

21. Groen A. E., 1997, *Three-dimensional elasto-plastic analysis of soils*, PhD Thesis, Delft University, 1-114

22. Herrmann H.J., Hansen A., Roux S., 1989, Fracture of disordered elastic lattices in two dimensions, *Physical Rev. B*, **39**, 637-647

23. Hilleborg A., 1985, The theoretical basis of a method to determine the fracture energy of concrete, *Materials and Structures*, **18**, 291-296

24. Hordijk D.A., 1991, *Local approach to fatigue of concrete*, PhD dissertation, Delft University of Technology

25. Ibrahimbegovic A., Markovic D., Gatuing F., 2003, Constitutive model of coupled damage-plasticity and its finite element implementation, *Eur. J. Finite Elem.*, **12**, 4, 381-405

26. Jirasek M., 1999, Comments on microplane theory, In: *Mechanics of Quasi-Brittle Materials and Structures*, G. Pijaudier-Cabot, Z. Bittnar and B. Gerard (edit.), Hermes Science Publications, 55-77

27. Jirasek M., 2004, Non-local damage mechanics with application to concrete, *Revue Francaise de Genie Civil.*, **8**, 683-707

28. Kozicki J., Tejchman J., 2006a, 2D lattice model for fracture in brittle materials, *Archives of Hydro-Engineering and Environmental Mechanics*, in press

29. Kozicki J., Tejchman J., 2006b, Measurements of the displacement field in concrete notched beams using a digital image correlation (DIC) technique, *Lecture, Int. Conf. EURO-C*, Mayrhofen

30. Lemaitre J., 1985, Coupled elasto-plasticity and damage constitutive equations, *Computer Methods Appl. Mech. Eng.*, **51**, 31-49

31. Menetrey P., Willam K.J., 1995, Triaxial failure criterion for concrete and its generalization, *ACI Structural Journal*, 311-318

32. Palaniswamy R., Shah S.P., 1974, Fracture and stress-strain relationship of concrete under triaxial compression, *J. Struct. Div. ASCE*, **100**, 901-916

33. Pamin J., 2004, *Gradient-Enchanced Continuum Models: Formulation, Discretization and Applications*, Habilitation Monography, Cracow University of Technology, Cracow

34. Pamin J., de Borst R., 1998, Simulation of crack spacing using a reinforced concrete model with an internal length parameter, *Arch. Appl. Mech.*, **68**, 9, 613-625

35. Pamin J., de Borst R., 1999, Stiffness degradation in gradient-dependent coupled damage-plasticity, *Arch. Mech.*, **51**, 3/4, 419-446

36. Peerlings R.H.J., de Borst R., Brekelmans W.A.M., Geers M.G.D., 1998, Gradient enhanced damage modelling of concrete fracture, *Mech. Cohesion.-Friction. Materials*, **3**, 323-342

37. Pietruszczak D., Jiang J., Mirza F.A., 1988, An elastoplastic constitutive model for concrete, *Int. J. Solids Structures*, **24**, 7, 705-722

38. Pijaudier-Cabot G., Bazant Z.P., 1987, Nonlocal damage theory, *ASCE J. Eng. Mech.*, **113**, 1512-1533

39. Sakaguchi H., Mühlhaus H.B., 1997, Mesh free modelling of failure and localisation in brittle materials, In: *Deformation and Progressive Failure in Geomechanics*, A. Asaoka, T. Adachi and F. Oka (edit.), 15-21

40. Salari M.R., Saeb S., Willam K., Patchet S.J., Carrasco R.C., 2004, A coupled elastoplastic damage model for geomaterials, *Computers Methods in Applied Mechanics and Engineering*, **193**, 2625-2643

41. Schlangen E., Garboczi E.J., 1997, Fracture simulations of concrete using lattice models: computational aspects, *Engineering Fracture Mechanics*, **57**, 319-332

42. Simone A., Wells G.N., Sluys L.J., 2002, Discontinuous modelling of crack propagation in a gradient enhanced continuum, *Proc. of the Fifth World Congress on Computational Mechanics, WCCM V*, Vienna, Austria

43. Sluys L., 1992, *Wave propagation, localisation and dispersion in softening solids*, PhD Thesis, Delft University of Technology

44. Sluys L.J., de Borst R., 1994, Dispersive properties of gradient and rate-dependent media, *Mech. Mater.*, **183**, 131-149

45. Tejchman J., 2006, Effect of fluctuation of current void ratio on the shear zone formation in granular bodies within micro-polar hypoplasticity, *Computers and Geotechnics*, **33**, 1, 1-68

46. Vervuurt A., van Mier J.G.M., Schlangen E., 1994, Lattice model for analyzing steel-concrete interactions, In: *Comp. Methods and Advances in Geomechanics*, Siriwardane and Zaman (edit.), 713-718, Balkema, Rotterdam

47. van Vliet M.R.A., van Mier J.G.M., 1996, Experimental investigation of concrete fracture under uniaxial compression, *Mechanics of Cohesive-Frictional Materials*, **1**, 115-127

48. Walukiewicz H., Bielewicz E., Gorski J., 1997, Simulation of nonhomogeneous random fields for structural applications, *Computers and Structures*, **64**, 1/4, 491-498

49. Willam K.J., Warnke E.P., 1975, Constitutive model for the triaxial behaviour of concrete, *IABSE Seminar on Concrete Structures Subjected to Triaxial Stress*, Bergamo, Italy, 1-31

50. Wittmann F.H., Mihashi H., Nomura N., 1992, Size effect on fracture energy using three-point bend tests, *Materials and Structures*, **25**, 327-334

Modelowanie lokalizacji odkształceń w materiałach quasi-kruchych z zastosowaniem modelu sprężysto-plastycznego

Streszczenie

W artykule przedstawiono wyniki symulacji numerycznych lokalizacji odkształceń w materiałach quasi-kruchych (jak beton) w płaskim stanie odkształcenia. Do opisu materiału przyjęto izotropowy model sprężysto-plastyczny-zniszczeniowy uwzględniający prawo sprężysto-plastyczne ze skalarną degradacją sztywności. W przypadku prawa sprężysto-plastycznego przyjęto kryterium plastyczności Druckera-Pragera w ściskaniu i kryterium plastyczności Rankine'a w rozciąganiu. Degradację sprężystą opisano z wykorzystaniem definicji odkształcenia zastępczego według warunku Rankine'a i wykładniczym prawem ewolucji. W celu otrzymania wyników niezależnych od siatki elementów skończonych, w obszarze osłabienia przyjęto teorię nielokalną. Przedstawiono wyniki symulacji numerycznych dla belki betonowej z nacięciem obciążonej dwoma siłami skupionymi. Wyniki numeryczne porównane z wynikami doświadczalnymi.

Manuscript received February 2, 2006; accepted for print July 6, 2006